

# EXPERIMENTAL AND MODELLING STUDIES ON THERMAL INSULATION AND SOUND ABSORPTION PROPERTIES OF CROSS-LAID NONWOVEN FABRICS

Tao Yang<sup>1,\*</sup>, Lizhu Hu<sup>2</sup>, Xiaoman Xiong<sup>3</sup>, Michal Petru<sup>1</sup>, Sundaramoorthy Palanisamy<sup>3</sup>, Kai Yang<sup>3</sup>, Jan Novák<sup>4</sup>, Jiří Militký<sup>3</sup>

1 Institute for Nanomaterials, Advanced Technologies and Innovation, Technical University of Liberec, 46117 Liberec, Czech Republic

2 Jiangxi Center for Modern Apparel Engineering and Technology, Jiangxi Institute of Fashion Technology, Nanchang, 330200, China

3 Department of Material Engineering, Faculty of Textile Engineering, Technical University of Liberec, Liberec 46117, Czech Republic

4 Department of Vehicles and Engines, Faculty of Mechanical Engineering, Technical University of Liberec, Liberec 46117, Czech Republic

\*Corresponding author. E-mail: tao.yang@tul.cz

## Abstract:

Nonwoven fabrics are widely used for thermal insulation and sound absorption purpose in construction and automobile fields. It is essential to investigate their thermal conductivity and sound absorption coefficient. Five cross-laid nonwoven fabrics are measured on the Alambeta device and Brüel & Kjær impedance tube. Bogaty and Bhattacharyya models are selected to predict the thermal conductivity, and Voronina and Miki models are used to predict the sound absorption coefficient. The predicted thermal conductivity shows a significant difference compared with the measured values. It is concluded that Bogaty and Bhattacharyya models are not suitable for high porous nonwoven fabric. In addition, the results of Voronina and Miki models for sound absorption prediction are acceptable, but Voronina model shows lower mean prediction error compared with Miki model. The results indicate that Voronina model can be used to predict the sound absorption of cross-laid nonwoven fabric.

## Keywords:

Thermal insulation; sound absorption; nonwoven; polyester

## 1. Introduction

In the background of worldwide energy saving and emission reduction, thermal insulation is very important for constructions and automobiles because it significantly affect the energy consumption and CO<sub>2</sub> emissions. Thermal insulation materials are still the major tool to improve a building's energy behavior after the introduction of compulsory thermal insulation in most European countries [1]. The most widely used insulation materials can be classified into two categories: foamy material and fibrous material. As a typical fibrous material, nonwoven fabrics are dominant in the market due to their high porosity, economical price, lightweight, flexible structure, good thermal insulation, etc. The thermal insulation properties of nonwoven fabric depends upon its volume fraction of air and its pore shape.

Nonwoven fabrics are not only good thermal insulators, but also ideal sound absorbers [2]. Sound absorbers can reduce noise and control the reverberation time to improve the acoustic comfort in concert halls, working places, exhibition halls, opera houses, etc. Energy loss of sound wave caused by viscous effects and thermal losses are primarily the mechanisms involved in sound absorption [3]. Such losses occur during sound propagation in the interconnected pores of a porous absorber. A thin layer of air adjacent to the wall of a pore is

where viscous losses happen. This is due to the viscosity of air, so sound dissipates with friction between the pore walls. The thermal conductivity of the air and the absorbent material has some impact on losses as well.

It has been investigated that thermal resistance and sound absorption properties of high porous nonwoven are correlated due to the strong dependence of these two properties on pore characteristics [4]. Porosity and pore geometry are the two critical parameters for thermal insulation and sound absorption. In the high porous material, the solid phase may not enough to form sufficient close pores. Consequently, an increase on porosity usually results in thermal resistance decrease. Meanwhile, as a result of porosity increase, less fibers involved in energy transfer from sound wave to absorber which means sound absorption performance declines. Other structure parameters also can significantly affect thermal insulation and sound absorption properties. For instance, the thermal resistance of airlaid nonwoven is not linear related to density, while the resistance increased exponentially with an initial increase in density, at that point leveled off and diminished directly with further increase in density [5]. The bulk density and sound absorption performance for the samples with similar thickness are strong related, and the increase of fabric areal density leads to an increase in sound absorption performance [6]. Thickness is also a key parameter for such properties. It



is well-known that thickness is a vital parameter for thermal insulation property of nonwoven fabric [7]. The increase in thickness results in an increased in sound absorption properties of nonwoven fabrics especially in low frequencies [6,8]. Besides, thermal insulation and acoustic absorption properties of nonwoven fabric can be affected by the fiber type and fiber size. Gibson et al. [9] investigated the effect of nanofibers on hybrid nonwoven materials. They found that nanofibers are more useful for high bulk density materials' thermal insulation and fiber diameter below 1  $\mu\text{m}$  are not thermally efficient at high porosity. However, nonwoven fabric containing more fine fibers usually has better sound absorption performance [10].

The theoretical estimation of thermal insulation and sound absorption properties of nonwoven fabrics are conventionally separately studied in literature. Manning and Panneton [11] used acoustic models to predict the sound absorption performance of Shoddy-based nonwoven fabrics. Soltani et al. [12] applied X-ray micro-computed tomography together with fluid simulation techniques to estimate the sound absorption properties of needled nonwoven fabrics. A simple simulation method was proposed for fibrous insulation materials design [13]. The researchers compared the thermal insulation performance of nonwoven fabrics with different fiber orientations.

Although the effect of structural parameters, fiber type and fiber size on thermal insulation and sound absorption properties have been well studied, there has been little quantitative analysis of numerical methods on these two properties. It is necessary and meaningful to study thermal insulation and sound absorption properties of nonwoven fabric since it can benefit energy saving and emission reduction in construction and automobile fields. Besides, it is necessary to figure out the suitability of several widely-used models on nonwoven fabrics. Thus, the main aim of this paper is to simultaneously investigate the thermal

insulation and sound absorption properties of nonwoven fabrics as well as the accuracy of some existing models.

## 2. Experimental

### 2.1. Materials

Five high-loft nonwoven fabrics were selected to carry out this study. The thermal conductivity and sound absorption were measured via Alambeta device and Brüel & Kjær impedance tube, respectively. The nonwoven fabrics are composed of 70 wt. % staple polyester fiber and 30 wt. % hollow polyester fiber. The nonwoven fabrics were developed on a Trützschler cross-lapper thermal bonding line. To produce webs that are particularly wide, thick and virtually isotropic, the cross-lapper precisely folds the web and lays it down in 4 to 15 layers at high speed. The Trützschler cross-lapper thermal bonding line utilizes through-air drying, in which hot air is used to bond webs made of fibers with different melting points. The thermo-bonder consists of a perforated drum, heating element and radial fan. The fan generates a suction draft, this results in heated air flowing from the oven chamber through the moist web. The airflow causes fibers with a low melting point to melt and the individual fibers stick together. The hollow polyester with a low melt temperature which is 110°C for thermal bonding purpose. The specifications of staple and hollow polyester fiber are shown in Table 1. The mean fiber diameter was determined according to measurements on randomly selected 312 fibers with a value of 22.905  $\mu\text{m}$ . The fiber density was measured by liquid pycnometer method [14]. Fibers randomly selected from the nonwoven were used to measure the mixed fiber density. The density has been measured five times with the value of 1171.665  $\text{kg/m}^3$ . Besides, the density of each fiber type has been measured, they are 1240.986  $\text{kg/m}^3$  and 1032.810  $\text{kg/m}^3$  for staple polyester and hollow polyester, respectively.

**Table 1.** Specifications of polyester fibers

Type of PET	Content wt. %	Density $\text{kg/m}^3$	Staple Length mm	Fineness dtex
Staple PET	70	1240.986	50	1.82
Hollow PET	30	1032.810	60	4.94

Note: PET is the polyethylene terephthalate fiber.

**Table 2.** Characteristics of nonwoven fabrics

Samples	A	B	C	D	E
Areal density ( $\text{g/m}^2$ )	150	200	250	300	1000
Thickness (mm)	20.938 (0.920)	23.404 (1.045)	29.586 (1.446)	26.802 (1.589)	61.832 (1.125)
Bulk density ( $\text{kg/m}^3$ )	7.164	8.546	8.450	11.193	16.173
Porosity (%)	99.389	99.271	99.279	99.045	98.620
Air permeability (mm/s)	2098 (91.214)	1128 (70.852)	1578 (66.483)	883 (15.232)	667 (27.586)

Note: The standard deviation of thickness and air permeability is reported in brackets.

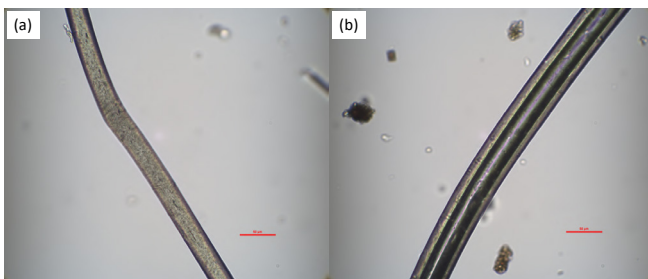


**Figure 1.** Longitudinal images of polyester fibers: (a) staple fiber; (b) hollow fiber

The longitudinal images of two types of polyester fibers are shown in Figure 1. The images were captured at the Technical University of Liberec (Liberec, Czech Republic) using the JENAPOL microscope (Jena, Germany) and NIS-elements software (AR 4.30.02 64-bit). The cross-sectional macroscopic images of polyester nonwoven fabric samples are illustrated in Figure 2, it can be seen that the fibers are cross-laid in the structure.

The characteristics of the nonwoven fabrics are listed in Table 2. Fabric thickness and areal density were determined according to ISO 9073-1:1989 [15]. The porosities of nonwoven fabrics were determined according to  $\epsilon = 1 - \rho/\rho_f$ , where  $\epsilon$  is the porosity,  $\rho_f$  is the fiber density, and  $\rho$  is the fabric bulk density [16]. The air permeability under 100 Pascal pressure drop is tested on the FX 3300 Textech Air Permeability Tester III at the Technical University of Liberec, Czech Republic. Each sample has been tested five times.

## 2.2. Measurement of thermal conductivity

The thermal conductivities of nonwoven fabrics were tested on an Alambeta device (SENSORA, Liberec, Czech Republic) at the Technical University of Liberec, Czech Republic. The measuring head of the Alambeta contains a copper block that is electrically heated to approximately 32 °C to simulate the temperature of human skin. The lower part of the heated block is equipped with a direct heat flow sensor that measures the thermal drop between the surfaces of a very thin, non-metallic plate using a multiple differential micro-thermocouple [17].

## 2.3. Impedance tube measurement

In this study, one impedance tube was used to obtain normal incidence sound absorption coefficient according to ISO 10534-2 [18]. A Brüel & Kjær measuring instrument containing Type 4206 Impedance Tube, PULSE Analyzer Type 3560, and Type 7758 Material Test Software was used for testing within the frequency range 50Hz - 6400 kHz. A large tube (100 mm in diameter) and a small tube (29 mm in diameter) were set up for measuring the sound absorption in low-frequency range (i.e. 50-1600Hz) and mid-to high-frequency range (i.e. 500-6400Hz) respectively. A schematic of the two microphone impedance tube setup used in this work is depicted in Figure 3. A sound source is mounted at one end of the impedance tube and the material sample is placed at the other end. The loudspeaker generates broadband, stationary random sound waves. These incident sound signals propagate as plane waves in the tube

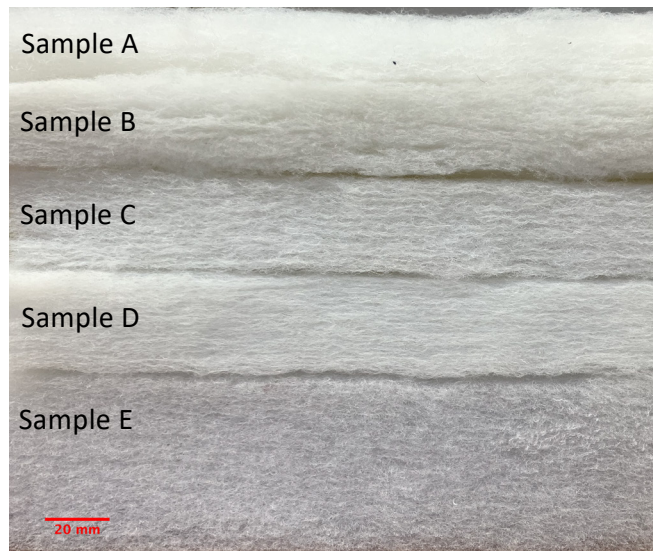


**Figure 2.** Cross-sectional macroscopic images of polyester nonwoven fabrics

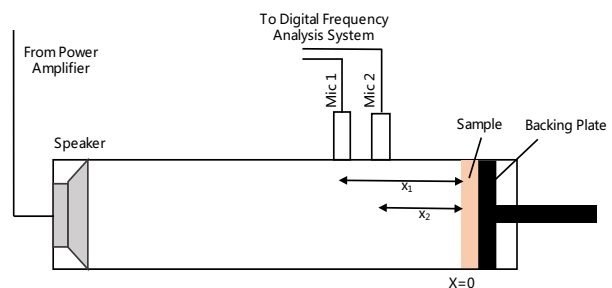


**Figure 3.** Two-microphone impedance tube schematic [19]

and hit the sample surface. The reflected wave signals are picked up and compared to the incident sound wave.

## 2.4. Thermal conductivity prediction

Theoretically, thermal conduction always occurs if a temperature gradient exists between a material system and the environment or inner a material system. The convection can be ignored due to the significant friction that is caused by constituent fibers against natural convection [20]. Sun and Pan stated that heat transfer via radiation can be eradicated when the temperature gradient is small [21]. Thus, thermal conduction is the dominant mechanism in most situations when heat is transferred through a nonwoven fabric.

Some models used to analyze the heat transfer behavior of fibrous materials are developed based on electrical network analysis which is called thermal-electrical analogy [22,23]. Two models used to predict the thermal conductivity of fibrous materials with fibers perpendicularly oriented the heat flow will be applied in this study. Bogaty [24] proposed one model for textile fabrics in 1957. In Bogaty model, the thermal conductivity for fibrous material with fibers perpendicularly oriented the heat flow is presented as:

$$k = \frac{k_f k_a}{k_a v_f + k_f v_a} \quad (1)$$

where  $k$  is the thermal conductivity,  $k_a$  is the thermal conductivity of air,  $k_f$  is the thermal conductivity of fiber,  $v_f$  is the volume fraction of fiber, and  $v_a$  is the volume fraction of air.

Bhattacharyya [25] presented two models to predict the thermal conductivity of samples with fibers perpendicularly and randomly to the heat flow. The Bhattacharyya model for fibrous material with fibers perpendicularly oriented the heat flow is presented as:

$$k = \left[ 1 - \frac{1 - k_a/k_f}{1 + \frac{2(k_a/k_f)(v_f/v_a)}{(1+k_a/k_f)}} \right] k_f \quad (2)$$

In these two models, the thermal conductivities and of volume fractions air and fiber should be known. All of the parameters are very easy to be obtained except thermal conductivity of fiber. The thermal conductivities of polyester are collected in one paper for thermal properties study of perpendicular-laid nonwoven fabrics [26]. The values of thermal conductivity of polyester fiber adopted in this study is  $0.140 \text{ W m}^{-1} \text{ K}^{-1}$  [27].

## 2.5. Sound absorption coefficient prediction

In the Zwicker and Kosten theory [28], the normal-incidence sound absorption coefficient,  $\alpha$ , is determined by the surface characteristic impedance:

$$\alpha = 1 - \left| \frac{\frac{Z_s - 1}{\rho_0 c_0}}{\frac{Z_s}{\rho_0 c_0} + 1} \right|^2 \quad (3)$$

where  $\rho_0$  is the air density at room temperature,  $c_0$  is the sound speed in air media at room temperature, and  $Z_s$  is the surface characteristic impedance:

$$Z_s = Z_c \coth(kl) \quad (4)$$

where  $Z_c$  is the characteristic impedance,  $k$  is the complex wavenumber, and  $l$  is the material thickness.

The empirical and semi-phenomenological models can estimate the characteristic impedance and complex wavenumber, the surface characteristic impedance and sound absorption coefficient can be further obtained. The procedure of sound absorption coefficient prediction is illustrated in Figure 4. The main difference between Voronina model and Miki model is that the airflow resistivity is required for Miki model and the latter requires porosity. Specific device is necessary to determine the airflow resistivity of nonwoven fabric, e.g., AFD300 AcoustiFlow (The Gesellschaft für Akustikforschung Dresden mbH, Dresden, Germany). It should be noted that airflow resistivity is a key parameter to the widely used impedance (or sound absorption) models, e.g., Delany–Bazley model, Garai–Pompoli model and Komatsu model [19]. Once the airflow resistivity is known, the impedance and sound absorption coefficient can be rapidly predicted based on the empirical models. Besides, the sound

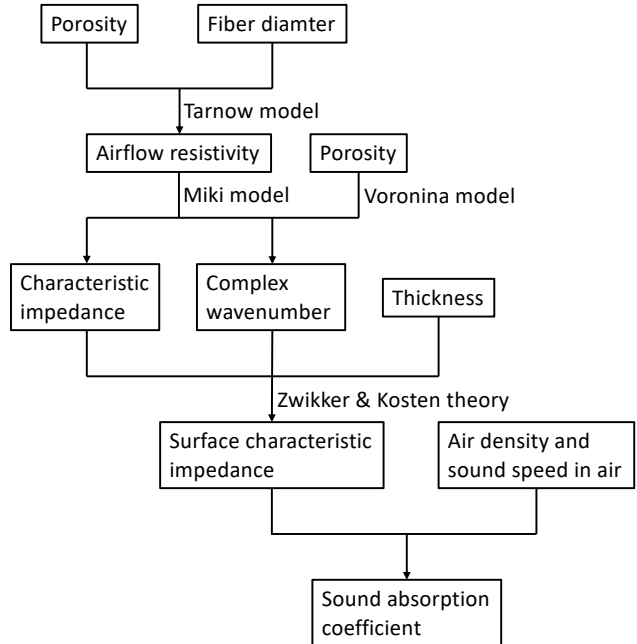


Figure 4. Procedure of sound absorption coefficient prediction

absorption performance of high porous nonwoven is generally proportionally correlated with airflow resistivity which means sound absorption performance is anticorrelated with air permeability.

Miki [29] developed a modification on the Delany-Bazley model [30] to generate a more accurate prediction, valid for a broader frequency range. The characteristic impedance and wavenumber in Miki's model are given by:

$$Z_c = \rho_0 c_0 \left( 1 + 0.0699 \left( \frac{f}{\sigma} \right)^{-0.632} - j 0.107 \left( \frac{f}{\sigma} \right)^{-0.632} \right) \quad (5)$$

$$k = \frac{\omega}{c_0} \left( 0.160 \left( \frac{f}{\sigma} \right)^{-0.618} + j \left( 1 + 0.109 \left( \frac{f}{\sigma} \right)^{-0.618} \right) \right) \quad (6)$$

where  $f$  is the frequency,  $\sigma$  is the airflow resistivity,  $j = \sqrt{-1}$  is the complex number, and  $\omega = 2\pi f$  is the angular frequency. The airflow resistivity can be estimated via numerical method. Some models used to estimate airflow resistivity are presented in Ref. 31. The airflow resistivity of nonwoven fabric is estimated according to one of the Tarnow models [32]:

$$\sigma = \frac{16\eta(1-\varepsilon)}{d^2 \{ \ln[(1-\varepsilon)^{-1/2}] - 0.5\varepsilon - 0.25\varepsilon^2 \}} \quad (7)$$

where  $\eta$  is the air dynamic viscosity,  $d$  is the mean fiber diameter, and  $\varepsilon$  is the porosity.

One model depending on porosity can be alternatively used to estimate sound absorption coefficient [33]. In this model, the characteristic impedance and the complex wavenumber is given by:

$$Z_c = \rho_0 c_0 (1 + Q - jQ) \quad (8)$$

$$k = \frac{\omega}{c_0} \left( \frac{Q(2+Q)}{1+Q} + j(1+Q) \right) \quad (9)$$

where  $Q$ , the structural characteristic, is:

$$Q = \frac{(1-\varepsilon)(1+q_0)}{\varepsilon d} \sqrt{\frac{4\eta}{\pi f \rho_0}} \quad (10)$$

where  $q_0$  is obtained from the following empirical expression:

$$q_0 = \frac{1}{1+2 \times 10^4 (1-\varepsilon)^2} \quad (11)$$

It was stated that this model is valid if the following condition is met,  $d \frac{2\pi f}{c_0} 10^4 > 0.5$ , which means the lower frequency limit  $f_{low}$  is:

$$f_{low} = \frac{c_0}{4\pi d} 10^{-4} \quad (12)$$

The lower frequency limit for the cross-laid nonwoven fabric is  $\sim 120$  Hz in current study. Hence, the comparison between predicted sound absorption and measured values will be conducted in the frequency range of 120 – 6400 Hz.

**Table 3.** Thermal conductivities of nonwoven fabrics

Samples	Measured thermal conductivity ( $\text{W m}^{-1} \text{K}^{-1}$ )	Predicted values thermal conductivity ( $\text{W m}^{-1} \text{K}^{-1}$ )	
		Bogaty model	Bhattacharyya model
A	0.0475 (0.0014)	0.0265	0.0266
B	0.0425 (0.0012)	0.0266	0.0267
C	0.0537 (0.0016)	0.0266	0.0267
D	0.0429 (0.0011)	0.0266	0.0267
E	0.1185 (0.0249)	0.0267	0.0269

Note: The standard deviation of measured thermal conductivity is reported in brackets.

### 3. Results and discussion

#### 3.1. Thermal conductivity

The measured and predicted thermal conductivities of nonwoven fabrics are listed in Table 2. Each sample has been measured five times on the Alambeta device. Sample B exhibits the lowest thermal conductivity, and sample E has the highest conductivity value. Except Sample E, all of the samples show acceptable standard deviation. This is due to the measurement uncertainties and large thickness of Sample E. The Alambeta device can rapidly test the thermal properties of fibrous materials by simulating the temperature of human skin. But the upper and lower heat flow sensors are open and free during test, so free convection and heat dissipation could occur at the edge of the specimen, especially for thick and high porous specimen.

From Table 3, it can be seen that predicted values have significant difference compared with the measured values. Moreover, the predicted values from two models are very close. In order to clearly compare the measured and predicted values and analyze the reason of nearly same predicted values, the thermal conductivities of nonwoven fabrics and the predicted thermal conductivities when the porosity ranges from 0 to 100% and from 90% to 100% are illustrated in Figure 5. The predicted value is based on the  $0.140 \text{ W m}^{-1} \text{K}^{-1}$  fiber thermal conductivity. It can be seen that the two models show very similar predictions when the sample has low porosity (i.e.  $< 10\%$ ) and high porosity (i.e.  $> 80\%$ ). Although Bhattacharyya model has higher predictions compared with Bogaty model, the mean difference for these two models are 14.69% in the whole porosity range. The porosities of most nonwoven fabric are usually higher than 90%. Also, the predicted thermal conductivities are respectively around  $0.0305 \text{ W m}^{-1} \text{K}^{-1}$  and  $0.0285 \text{ W m}^{-1} \text{K}^{-1}$  for Bogaty model and Bhattacharyya model when the porosity is 90%, and the change of thermal conductivity is insignificant in the porosity range of 98-100%. If the porosity is between 10% and 80% the fiber volume fraction plays an important role on the thermal conductivity in these two models. But in current study, porosity of the samples ranges from 98.620% to 99.389%. Hence, the predicted values for the nonwoven fabrics are very close and lower than the measured

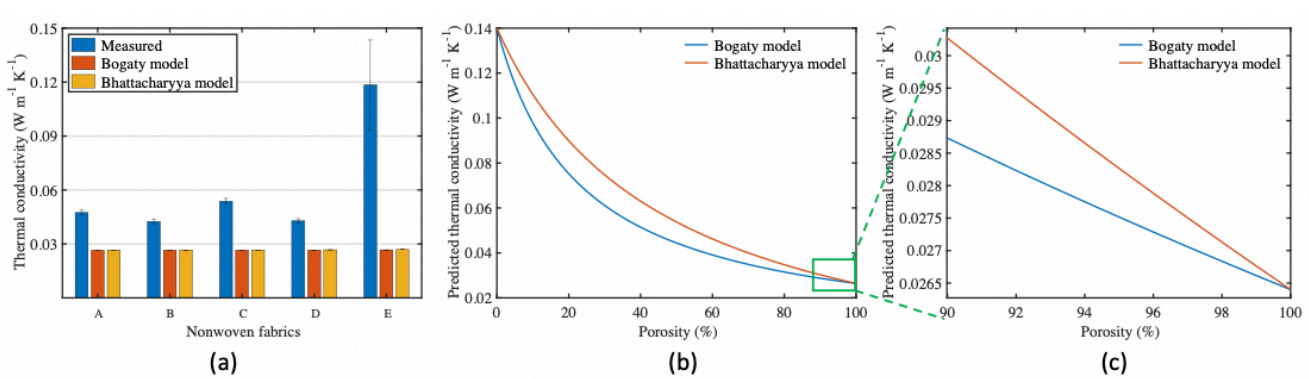


**Figure 5.** The measured and predicted thermal conductivities: (a) comparison between measured and predicted values; (b) predicted values for the porosity ranges from 0 to 100 %; (c) predicted values for the porosity ranges from 90 % to 100 %

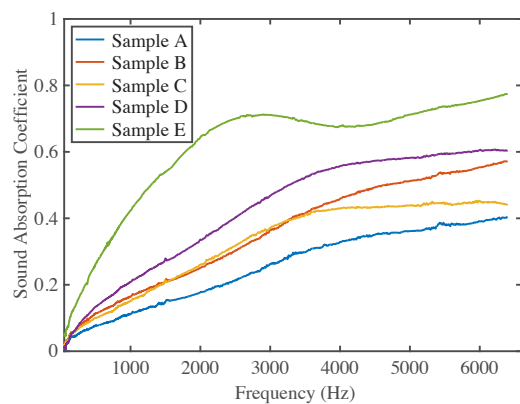


**Figure 6.** Sound absorption coefficient of nonwoven fabrics in 50 – 6400 Hz frequency range

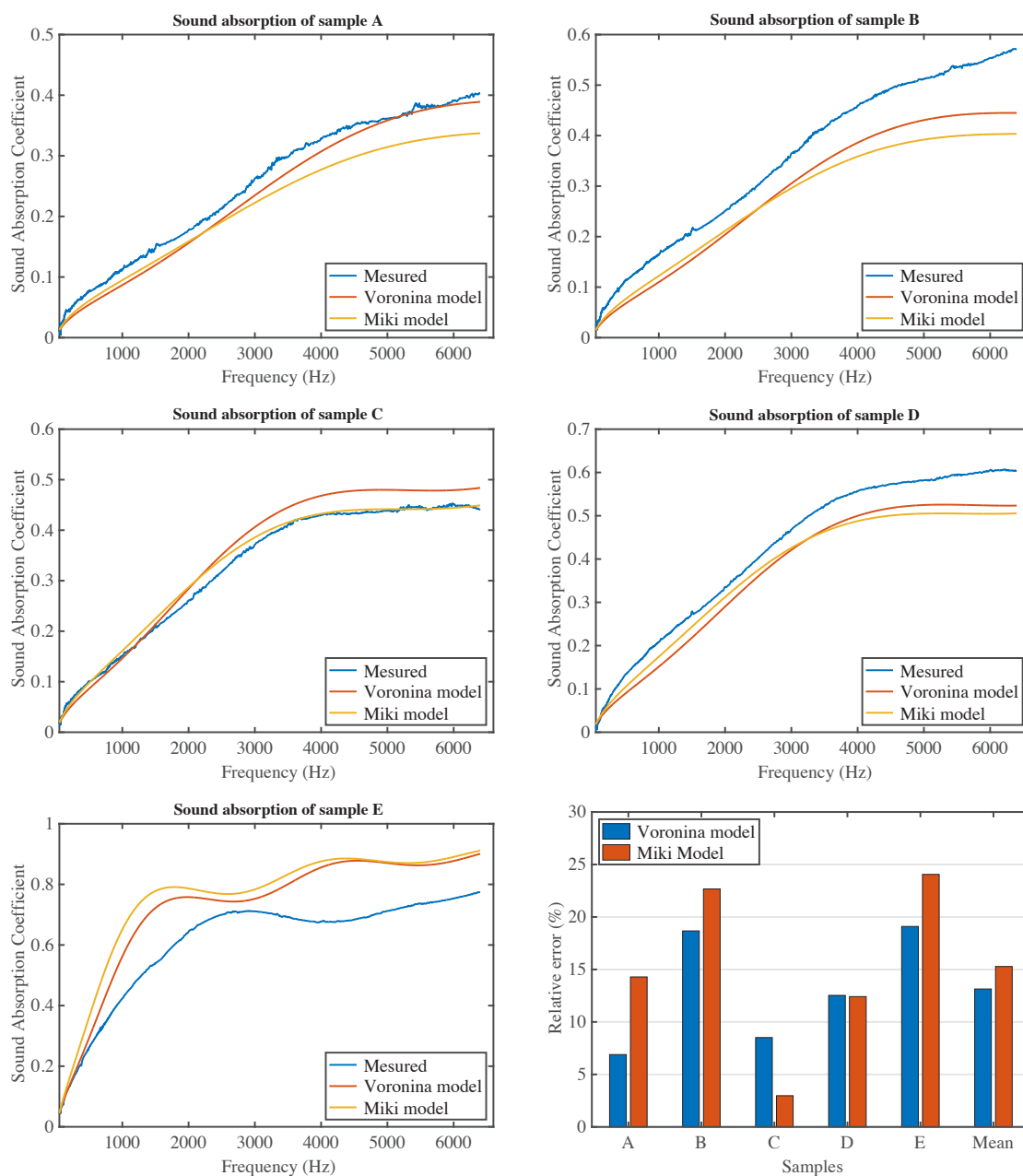


**Figure 7.** Comparison between measured and predicted sound absorption coefficient, and the relative error of Voronina and Miki models

values. It can be concluded that the Bogaty and Bhattacharyya models are not suitable for high porous nonwoven fabrics.

### 3.2. Sound absorption

The normal incidence sound absorption coefficient of nonwoven fabric is showed in Figure 6. The sound absorption is determined as a function of frequency. The measured data in the low frequencies of 50-1600 Hz (using the Type 4206 large tube) and the high frequencies of 500-6400 Hz (using the Type 4206 small tube) were combined together to form the curves. Samples A, B, C and D have low sound absorption coefficient in low frequencies. The highest absorption coefficient of these four samples is around 0.6. Sample E exhibits a relatively good sound absorption performance. For small thickness samples, the sound absorption coefficient increases with the increase in frequency. However, sound absorption coefficient of thick samples show fluctuations with increasing frequency by reason

of resonance phenomena. This can explain the behavior of the sound absorption curves in Figure 6. In addition, Sample B and Sample C have similar absorption performance at the frequency lower than approximate 3500 Hz but Sample B exhibits better performance in the high frequency range. This is due to the thickness and density differences. Sample B has higher density but smaller thickness compared with Sample C. Thickness is more significant at low frequencies and higher density usually results in higher airflow resistivity and lower air permeability.

The comparisons between measured sound absorption and predicted value of each sample are demonstrated in Figure 7. It is hard to conclude that which model is more suitable for nonwoven fabric by observation on each sample. The Voronina model shows a good prediction for Sample A, while the Miki model has a good agreement on Sample C. Nevertheless, both Voronina and Miki models under- or overestimate the measured values of Samples B, D and E. The overestimation on prediction of Sample E is most obvious. To numerically investigate the accuracy of Voronina and Miki models, the relative prediction error  $\Delta$  was determined according to the following equation:

$$\Delta = \frac{|\bar{\alpha}_m - \bar{\alpha}_p|}{\bar{\alpha}_m} \times 100\% \quad (13)$$

where  $\bar{\alpha}_m$  and  $\bar{\alpha}_p$  are respectively the mean value of measured and predicted sound absorption coefficient in the frequency range of 120 - 6400 Hz. The mean relative error is the average value of five samples. Lower relative prediction error means the prediction is more accurate.

The relative error of Miki model is in the range of 2.971 - 24.055%. The prediction of Voronina model is more stable than Miki model. The most accurate prediction of Miki model is occurred on Sample C with the lowest relative error, while the errors for Samples B and E are over than 20%. Moreover, the mean relative error of Voronina model is smaller than the value of Miki model. It has been reported that Miki model is more suitable for multi-component polyester nonwoven fabric [16], but the Voronina model is more accurate than Miki model in this study. This can be attributed to the possible error on airflow resistivity estimation. As stated above, the airflow resistivity is critical for Miki model. One Tarnow model was adopted to estimate the airflow resistivity of nonwoven fabric. Although the Tarnow model has been proven that it is reliable for fibrous material, it is not 100% accurate for all types of nonwoven fabric. Additionally, the mean relative error of Voronina model is 13.14% which is acceptable for high porous nonwoven fabric.

#### 4. Conclusions

In this work, the thermal insulation and sound absorption properties of nonwoven fabrics have been experimentally and numerically studied. The Alambeta device and Brüel & Kjær impedance tube were used to respectively carry out the measurements on thermal conductivity and sound absorption coefficient. Bogaty and Bhattacharyya models were selected to predict the thermal conductivity. The sound absorption coefficient were predicted based on Voronina and Miki models.

The results indicate that both Bogaty and Bhattacharyya models are not suitable for the materials having high porosity (e.g. > 98%) since these two models assumed that the heat transfer via air is dominant if the air volume fraction is much bigger than fiber volume fraction. Sample E exhibited the best sound absorption performance among all of the samples. But the absorption curve of Sample E was fluctuated due to the resonance phenomena. It was found that Voronina model is more accurate than Miki model if the airflow resistivity measurement is absent. Thus, it can be concluded that the Voronina model can be used to predict the sound absorption coefficient of nonwoven fabric when the airflow measurement is not available.

The insights gained from this study may be of assistance to understanding the thermal insulation and acoustic absorption properties of nonwoven fabric as well as the suitability of several models. A limitation of this is study is that the presented two models didn't show an acceptable prediction on thermal conductivity. Hence, further work need to be done to establish a more acceptable model to accurately predict the thermal properties of high porous nonwoven fabrics.

#### ACKNOWLEDGEMENTS

This article is based upon work from the European Union (European Structural and Investment Funds - Operational Programme Research, Development and Education) in the frames of the project "Modular platform for autonomous chassis of specialized electric vehicles for freight and equipment transportation", Reg. No. CZ.02.1.01/0.0/0.0/16\_025/0007293. The authors would like to thank Ms. Shiyi Jin, Ms. Tianshu Li and Ms. Ting Long for their help throughout the measurements. The authors would like to thank Dr. Rajesh Mishra for his valuable suggestion in revision. Tao Yang would like to thank Dr. Jana Salacova and Ms. Jana Stranska for their guide on fibers and fabrics characterization.

#### References

- [1] Papadopoulos, A. M. (2005). *State of the Art in Thermal Insulation Materials and Aims for Future Developments*. *Energy and Buildings*, 37.(1.), 77–86.
- [2] Patnaik, A., Mvubu, M., Muniyasamy, S., Botha, A., Anandjiwala, R. D. (2015). *Thermal and Sound Insulation Materials from Waste Wool and Recycled Polyester Fibers and Their Biodegradation Studies*. *Energy and Buildings*, 92., 161–169.
- [3] Cox T. J., D'Antonio, P. (2009). *Acoustic absorbers and diffusers: Theory, design and application* (2 ed). Taylor & Francis (New York).
- [4] Yang, T., Xiong, X., Mishra, R., Novák, J., Milíký, J. (2018). *Acoustic Evaluation of Struto Nonwovens and Their Relationship with Thermal Properties*. *Textile Research Journal* 88.(4.), 426–37.
- [5] Cerkez, I., Kocer, H. B., Broughton, R. M. (2018). *Airlaid Nonwoven Panels for Use as Structural Thermal Insulation*. *Journal of the Textile Institute*, 109.(1.), 17–23.

[6] Yang, T., Xiong, X., Mishra, R., Novák, J., Militký, J. (2019). Sound Absorption and Compression Properties of Perpendicular-Laid Nonwovens. *Textile Research Journal*, 89.(4.), 612–624.

[7] Martin, J. R., Lamb, G. E. R. (1987). Measurement of Thermal Conductivity of Nonwovens Using a Dynamic Method. *Textile Research Journal*, 57.(12.), 721–727.

[8] Küçük, M., Korkmaz, Y. (2012). The Effect of Physical Parameters on Sound Absorption Properties of Natural Fiber Mixed Nonwoven Composites. *Textile Research Journal*, 82.(20.), 2043–2053.

[9] Gibson, P., Lee, C. (2004). Application of Nanofiber Technology to Nonwoven Thermal Insulation. *Proceedings of 14th Annual International TANDEC Nonwovens Conference*, 2.(2.), 1–14.

[10] Lee, Y., Joo, C. (2003). Sound Absorption Properties of Recycled Polyester Fibrous Assembly Absorbers. *Autex Research Journal*, 3.(2.), 78–84.

[11] Manning, J., Panneton, R. (2013). Acoustical Model for Shoddy-Based Fiber Sound Absorbers. *Textile Research Journal*, 83.(13.), 1356–1370.

[12] Soltani, P., Azimian, M., Wiegmann, A., Zarrebini, M. (2018). Experimental and Computational Analysis of Sound Absorption Behavior in Needled Nonwovens. *Journal of Sound and Vibration*, 426., 1–18.

[13] Arambakam, R., Tafreshi, H. V., Pourdeyhimi, B. (2013). A Simple Simulation Method for Designing Fibrous Insulation Materials. *Materials and Design*, 44., 99–106.

[14] Maciel, N. de O. R., Ribeiro C. G. D., Ferreira, J., Vieira, J. da S., Marciano, C. R., Vieira, C. M., Margem, F. M., Monteiro, S. N. (2017). Comparative Analysis of Curaua Fiber Density Using the Geometric Characterization and Pycnometry Technique. In: Ikhmayies, S., Li, B., Carpenter, J. S., Li, J., Hwang, J.-Y., Monteiro, S.N., Firrao, D., Zhang, M., Peng, Z., Escobedo-Diaz, J.P., Bai, C., Kalay, Y.E., Goswami, R., Kim, J. (Eds.) *Characterization of Minerals, Metals, and Materials*. Cham: Springer International Publishing (Cham).

[15] ISO 9073-1:1989. *Textiles -- Test methods for nonwovens -- Part 1: Determination of mass per unit area*.

[16] ASTM C830-00: 2000. *Standard test methods for apparent porosity, liquid absorption, apparent specific gravity, and bulk density of refractory shapes by vacuum pressure*.

[17] Hes, L., de Araujo, M., Djulay, V.V. (1996). Effect of Mutual Bonding of Textile Layers on Thermal Insulation and Thermal Contact Properties of Fabric Assemblies. *Textile Research Journal*, 66., 245–250.

[18] ISO10534-2:1998. *Determination of sound absorption coefficient and impedance in impedance tubes, Part 2: Transfer-function method international organization for standardization*.

[19] Yang, T., Saati, F., Horoshenkov, K. V., Xiong, X., Yang, K., Mishra, R., Marburg, S., Militký, J. (2019). Study on the Sound Absorption Behavior of Multi-Component Polyester Nonwovens: Experimental and Numerical Methods. *Textile Research Journal* 89.(16.), 3342–3361.

[20] Sun, Z. Pan, N. (2006) *Thermal conduction and moisture diffusion in fibrous materials*. In: Pan, N., Gibson, P. (Ed.). *Thermal and moisture transport in fibrous materials*, Woodhead Publishing Ltd (Cambridge).

[21] Arambakam, R., Tafreshi, H. V., Pourdeyhimi, B. (2014). Modeling performance of multi-component fibrous insulations against conductive and radiative heat transfer. *International Journal of Heat and Mass Transfer* 71., 341–348.

[22] Lawson, D. I., McGuire, J. H. (1953). *The Solution of Transient Heat-flow Problems by Analogous Electrical Networks*. *Proceedings of the Institution of Mechanical Engineers* 167., 275–290.

[23] Fricke, H. I. J. (1924). *A Mathematical Treatment of the Electrical conductivity and Capacity of Disperse Systems*. *Physical Review* 24., 678–681.

[24] Bogaty, H., Hollies, N. R. S., Harris, M. (1957). Some Thermal Properties of Fabrics: Part I: The Effect of Fiber Arrangement. *Textile Research Journal*, 27., 445–449.

[25] Bhattacharyya, R. K. (1980). Heat Transfer Model for Fibrous Insulations. In: MeElroy, D. L., Tye, R. P. (Ed.). *Thermal Insulation Performance, ASTM STP718*; American Society for Testing and Materials (West Conshohocken). pp. 272–286.

[26] Yang, T., Xiong, X., Petrù, M., Tan, X., Kaneko, H., Militký, J. (2020). Theoretical and Experimental Studies on Thermal Properties of Polyester Nonwoven Fibrous Material. *Materials* 13., 1–20.

[27] Baxter, S. (1946). *The Thermal Conductivity of Textiles*. *Proceedings of the Physical Society* 58., 105–118.

[28] Zwikker, C., Kosten, C. W. (1949). *Sound Absorbing Materials*. Elsevier (New York).

[29] Miki, Y. (1990). Acoustical properties of porous materials- Modification of Delany-Bazley models. *Journal of Acoustic Society of Japan*, 11.(1.), 19–24.

[30] Delany, M. E., Bazley, E. N. (1970). Acoustical properties of fibrous absorbent materials. *Applied Acoustics*, 3.(2.), 105–116.

[31] Yang, T., Mishra, R., Horoshenkov, K. V., Hurrell, A., Saati, F., Xiong, X. (2018). A Study of Some Airflow Resistivity Models for Multi-Component Polyester Fiber Assembly. *Applied Acoustics*, 139., 75–81.

[32] Tarnow, V. (1996). Airflow Resistivity of Models of Fibrous Acoustic Materials. *Journal of the Acoustical Society of America* 100., 3706–3713.

[33] Voronina, N. (1994). Acoustic properties of fibrous materials. *Applied Acoustics* 42.(2.), 165–174.